Support Information

Understanding The Role of Cl Doping in Oxygen Evolution Reaction on Cuprous Oxide by DFT

Hai-Hang Chen[a], Yongfei Ji[b], and Ting Fan*[a]*

[a] School of Chemistry and Chemical Engineering, South China University of Technology,

Guangzhou 510641, P. R. China

[b] School of Chemistry and Chemical Engineering, Guangzhou University,

Guangzhou 510006, P. R. China

E-mail address: tingfan@scut.edu.cn; yongfeiji2018@gzhu.edu.cn

Gibbs Free Energy Calculation

The Gibbs reaction free energy change ($\triangle G$) of each elementary step was based on the computational hydrogen electrode (CHE) model developed by Nørskov et al.[1] in which the energy of $H^+ + e^-$ pair is related to the energy of the H_2 gas and the potential. The thermodynamic correction was considered by the frequency calculation. Table S1 lists the zero-point energy corrections and entropic contributions of gaseous and intermediates adsorption on the goal substrates computed from their vibration frequencies in harmonic approximation. The gas-phase molecules are treated as an ideal gas.

Based on the four-electron reaction mechanism of OER, the change of Gibbs free energy for each elementary step of OER ($\triangle G_1$, $\triangle G_2$, $\triangle G_3$, and $\triangle G_4$) can be calculated by the following formulas:

$$\triangle G_1 = G(*OH) \tag{S1}$$

$$\triangle G_2 = G(*O) - G(*OH) \tag{S2}$$

$$\triangle G_3 = G(*OOH) - G(*O) \tag{S3}$$

$$\triangle G_4 = 4.92 \text{ eV} - G(*OOH) \tag{S4}$$

The step with the highest $\triangle G$ is the rate-determining step (RDS) of the OER is:

$$G^{OER} = \max[\triangle G_1, \triangle G_2, \triangle G_3, \triangle G_4] \tag{S5}$$

The overpotential of OER can be evaluated from the following formula:

$$\eta = (G^{OER} / e) - 1.23 \text{ V} \tag{S6}$$

Table S1 Zero-point energy corrections and entropic contributions of gaseous and intermediates adsorption on substrates.

	ZPE(eV)	TS(eV)
$H_2O(l)$	0.56	0.67
$H_2(g)$	0.27	0.41
*OH	0.35	0
*O	0.05	0
*OOH	0.41	0

Table S2 Convergence test of the K-POINTS for 2 × 2 supercell Cu_2O (111).

K-POINTS	Total energy (eV)	ΔE/atom (eV)
(1,1,1)	-443.35487	
(2,2,1)	-443.56154	0.00172
(3,3,1)	-443.56167	0.00000
(4,4,1)	-443.56135	0.00000

Table S3 Convergence test of the vacuum layer for 2 × 2 supercell Cu_2O (111).

Vacuum layer (nm)	Total energy (eV)	ΔE/atom (eV)
0.12	-443.58416	
0.13	-443.56154	0.00019
0.14	-443.56907	0.00006
0.15	-443.56778	0.00001

Table S4 Convergence test of the plane-wave cutoff energy of Cu_2O (111) unit cell.

Plane-wave cutoff energy (eV)	Total energy (eV)	ΔE/atom (eV)
510	-110.87961	
520	-110.88643	0.00006
530	-110.88575	0.00001

Table S5 Gibbs reaction free energy changes ($\triangle G$) of each intermediates and elementary step and overpotential (η) on the active sites of different $Cu_2O(111)$ surfaces. The numbers in red means that the potential-determining step $\triangle G$. The numbers in brackets mean the coordination number of intermediates.

Active sites	$\triangle G_{*OH}$ (eV)	$\triangle G_{*O}$ (eV)	$\triangle G_{*OOH}$ (eV)	$\triangle G_1$ (eV)	$\triangle G_2$ (eV)	$\triangle G_3$ (eV)	$\triangle G_4$ (eV)	$\eta(V)$
1-$Cu_2O(111)$	0.56 (2)	1.74 (3)	3.91 (2)	0.56	1.18	2.16	1.01	0.93
2-$Cu_2O(111)$	0.63 (2)	2.00 (3)	4.18 (2)	0.63	1.37	2.18	0.74	0.95
3-$Cu_2O(111)$	0.86 (2)	1.92 (3)	4.05 (2)	0.86	1.05	2.13	0.87	0.90
1-Cl-$Cu_2O(111)$	-0.34 (2)	1.16 (3)	3.27 (2)	-0.34	1.50	2.11	1.65	0.88
2-Cl-$Cu_2O(111)$	-0.12 (2)	1.26 (3)	3.31 (2)	-0.12	1.39	2.05	1.61	0.82
3-Cl-$Cu_2O(111)$	-0.37 (2)	1.20 (3)	3.11 (2)	-0.37	1.57	1.91	1.81	0.68
4-Cl-$Cu_2O(111)$	-0.23 (2)	1.17 (3)	3.28 (2)	-0.23	1.39	2.12	1.64	0.89
5-Cl-$Cu_2O(111)$	-0.12 (2)	1.26 (3)	3.32 (2)	-0.12	1.38	2.06	1.60	0.83
6-Cl-$Cu_2O(111)$	-0.32 (2)	1.16 (3)	3.21 (2)	-0.32	1.48	2.05	1.71	0.82
7-Cl-$Cu_2O(111)$	-0.12 (2)	1.68 (3)	3.32 (2)	-0.12	1.81	1.63	1.60	0.58

8-Cl-Cu$_2$O(111)	-0.32 (2)	1.15 (3)	3.21 (2)	-0.32	1.48	2.06	1.71	0.83
9-Cl-Cu$_2$O(111)	0.19 (2)	1.73 (3)	3.58 (2)	0.19	1.54	1.84	1.34	0.61
10-Cl-Cu$_2$O(111)	0.08 (2)	1.54 (3)	3.54 (2)	0.08	1.46	1.99	1.38	0.76
11-Cl-Cu$_2$O(111)	0.04 (2)	1.26 (3)	3.53 (2)	0.04	1.22	2.27	1.39	1.04
1-V$_{Cu}$-Cu$_2$O(111)	1.77 (2)	2.83 (3)	5.07 (2)	1.77	1.06	2.24	-0.15	1.01
1'-V$_{Cu}$-Cu$_2$O(111)	1.79 (3)	2.83 (3)	5.31 (3)	1.79	1.03	2.48	-0.39	1.25
2-V$_{Cu}$-Cu$_2$O(111)	1.50 (2)	3.25 (2)	4.80 (2)	1.50	1.75	1.55	0.12	0.52
1-V$_{Cu}$-Cl-Cu$_2$O(111)	1.25 (2)	2.85 (2)	4.70 (2)	1.25	1.60	1.84	0.22	0.61
1'-V$_{Cu}$-Cl-Cu$_2$O(111)	1.58 (3)	2.78 (3)	4.74 (3)	1.58	1.20	1.95	0.18	0.72
2-V$_{Cu}$-Cl-Cu$_2$O(111)	1.57 (2)	3.26 (2)	4.82 (2)	1.57	1.69	1.55	0.10	0.46
3-V$_{Cu}$-Cl-Cu$_2$O(111)	1.48 (2)	3.21 (2)	4.71 (2)	1.48	1.73	1.50	0.21	0.50
4-V$_{Cu}$-Cl-Cu$_2$O(111)	1.74 (2)	2.81 (3)	5.02 (2)	1.74	1.07	2.21	-0.10	0.98
5-V$_{Cu}$-Cl-Cu$_2$O(111)	1.48 (2)	3.21 (2)	4.80 (2)	1.48	1.72	1.59	0.12	0.49

Table S6 Interaction/distortion analysis after OH/OOH adsorption on sites 1 and 2 of V_{Cu}-$Cu_2O(111)$ and V_{Cu}-Cl-$Cu_2O(111)$ (eV). The numbers in brackets mean the coordination number of intermediates.

Surface	Intermediates	E_{dist}(Surf)	E_{dist}(OH/O/OOH)	E_{int}	E_{ads}
1-V_{Cu}-$Cu_2O(111)$	*OH(2)	0.31	0.00	-2.22	-1.91
1-V_{Cu}-$Cu_2O(111)$	*O(3)	0.59	0.00	-3.70	-3.10
1-V_{Cu}-$Cu_2O(111)$	*OOH(2)	0.22	0.18	-0.80	-0.40
1-V_{Cu}-Cl-$Cu_2O(111)$	*OH(2)	1.42	0.00	-3.86	-2.44
1'-V_{Cu}-Cl-$Cu_2O(111)$	*O(3)	0.64	0.00	-3.79	-3.15
1-V_{Cu}-Cl-$Cu_2O(111)$	*OOH(2)	1.36	0.30	-2.39	-0.73
2-V_{Cu}-$Cu_2O(111)$	*OH(2)	0.28	0.00	-2.46	-2.18
2-V_{Cu}-$Cu_2O(111)$	*O(2)	0.54	0.00	-3.22	-2.68
2-V_{Cu}-$Cu_2O(111)$	*OOH(2)	0.20	0.16	-1.02	-0.66
2-V_{Cu}-Cl-$Cu_2O(111)$	*OH(2)	0.32	0.00	-2.44	-2.11
2-V_{Cu}-Cl-$Cu_2O(111)$	*O(2)	0.47	0.00	-3.14	-2.67
2-V_{Cu}-Cl-$Cu_2O(111)$	*OOH(2)	0.21	0.15	-1.02	-0.65
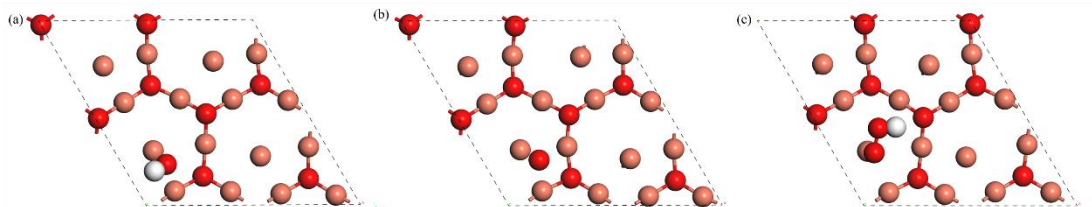
Fig. S1 The optimized adsorbed intermediates of (a) *OH, (b) *O, and (c) *OOH on active site 1 of $Cu_2O(111)$.
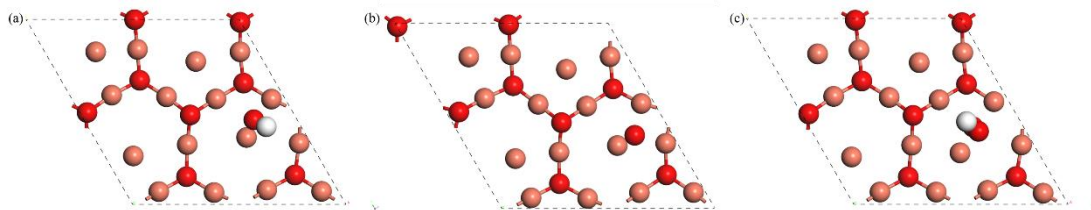
Fig. S2 The optimized adsorbed intermediates of (a) *OH, (b) *O, and (c) *OOH on active site 2 of Cu$_2$O(111).
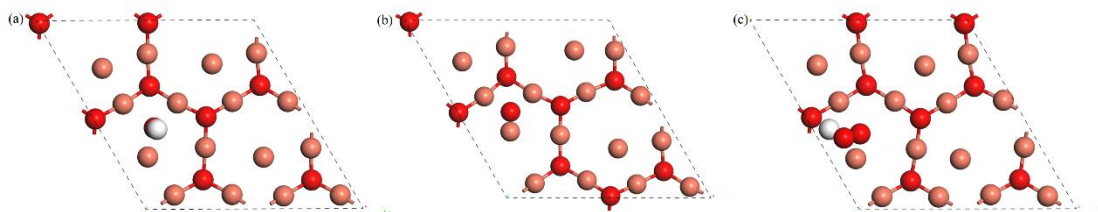
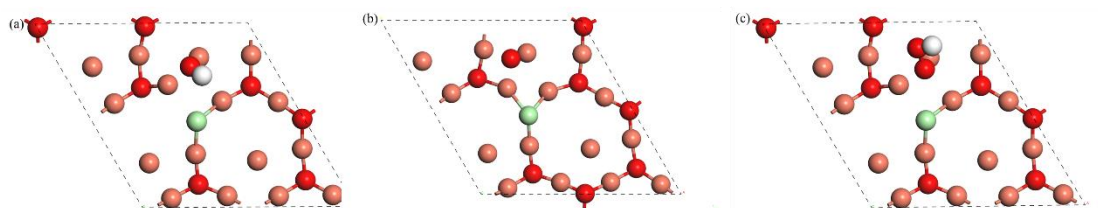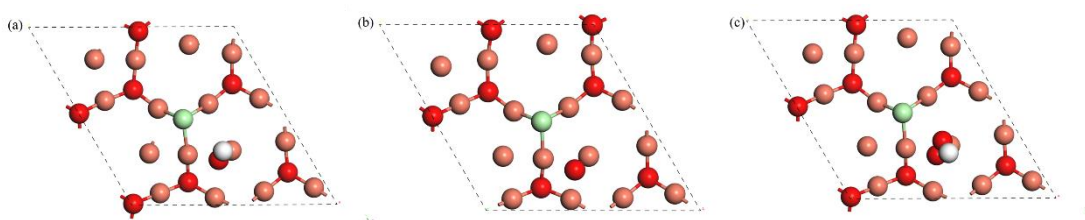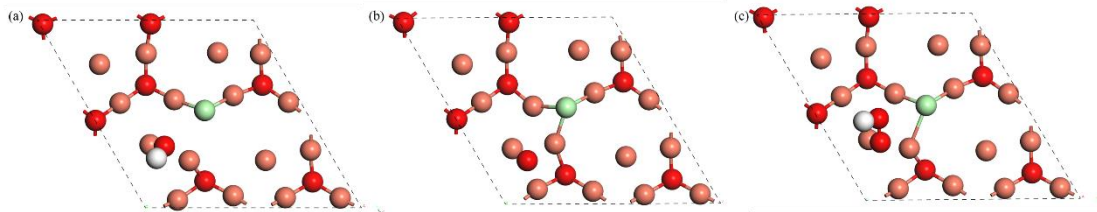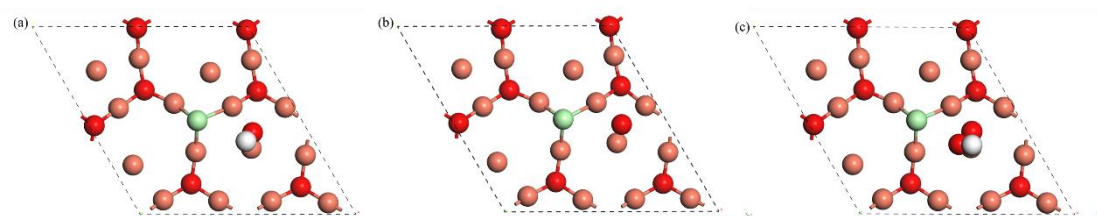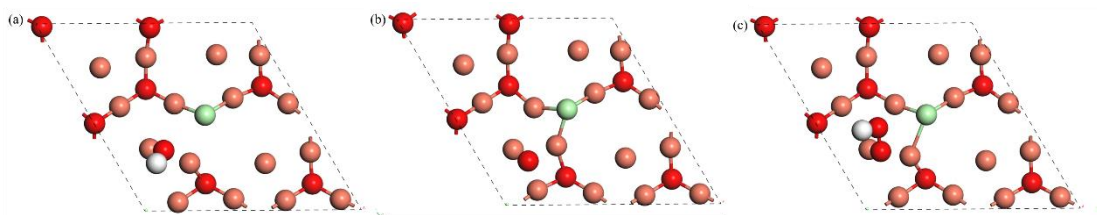**Fig. S3** The optimized adsorbed intermediates of (a) *OH, (b) *O, and (c) *OOH on active site 3 of Cu$_2$O(111).
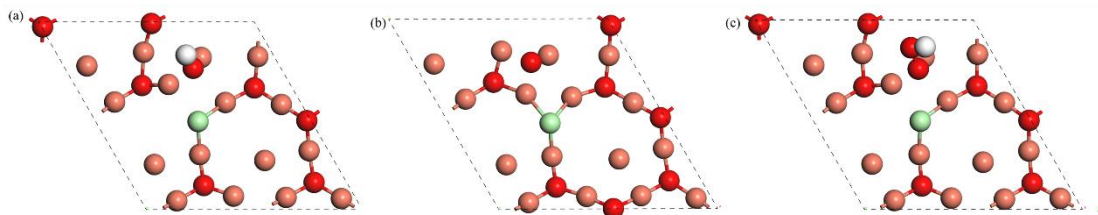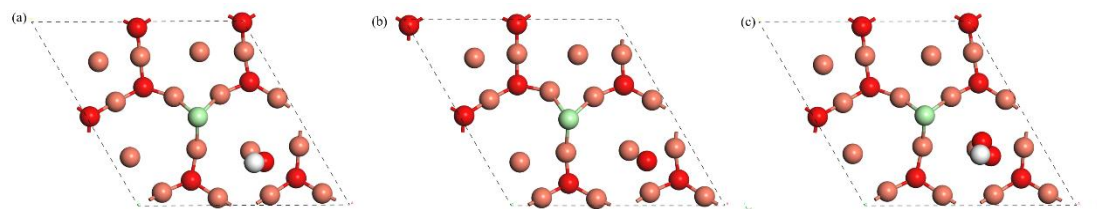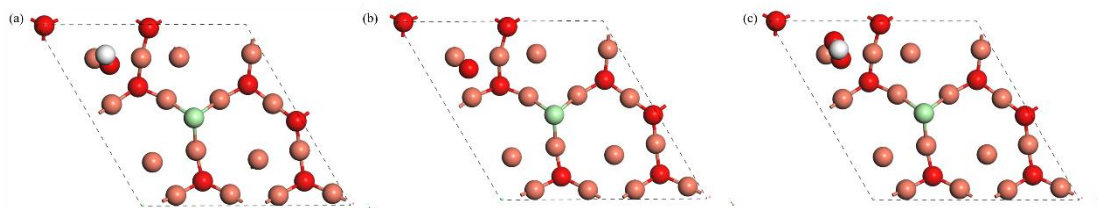

Fig. S4 The optimized adsorbed intermediates of (a) *OH, (b) *O, and (c) *OOH on active site 1 of Cl-Cu$_2$O(111).
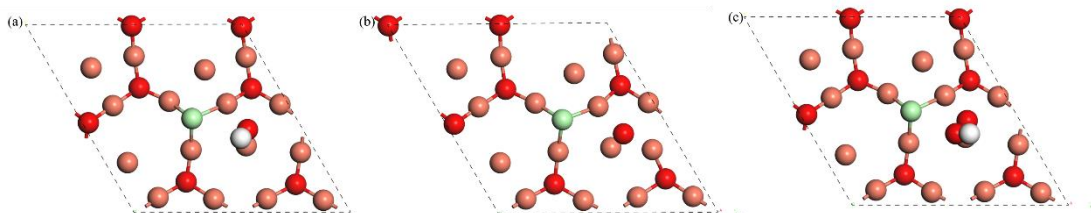
Fig. S5 The optimized adsorbed intermediates of (a) *OH, (b) *O, and (c) *OOH on active site 2 of Cl-Cu$_2$O(111).
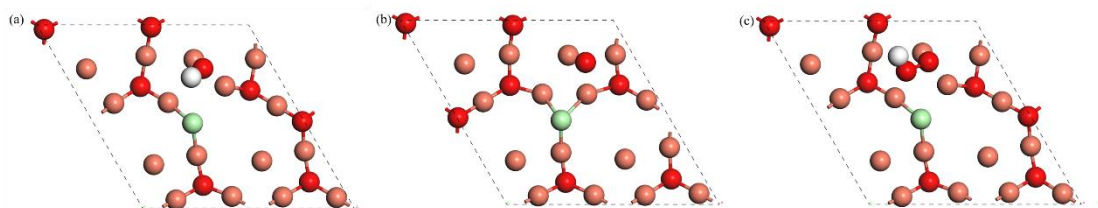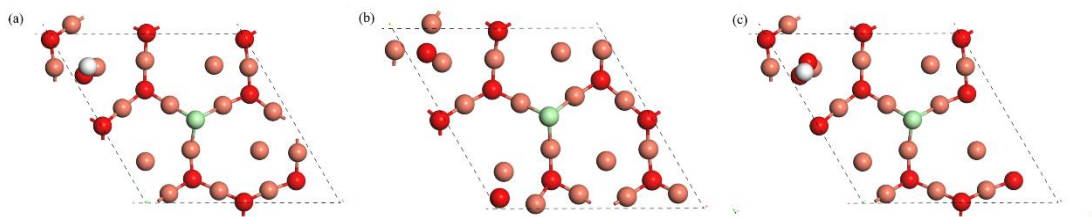

Fig. S6 The optimized adsorbed intermediates of (a) *OH, (b) *O, and (c) *OOH on active site 3 of Cl-Cu$_2$O(111).

Fig. S7 The optimized adsorbed intermediates of (a) *OH, (b) *O, and (c) *OOH on active site 4 of Cl-Cu$_2$O(111).

Fig. S8 The optimized adsorbed intermediates of (a) *OH, (b) *O, and (c) *OOH on active site 5 of Cl-Cu$_2$O(111).

Fig. S9 The optimized adsorbed intermediates of (a) *OH, (b) *O, and (c) *OOH on active site 6 of Cl-Cu$_2$O(111).
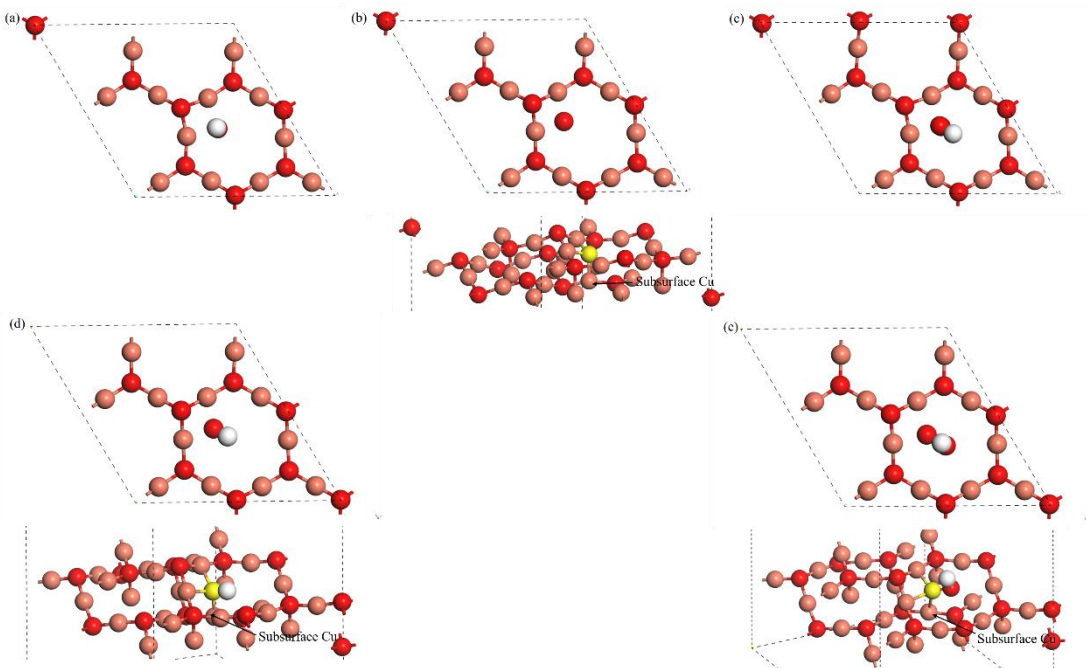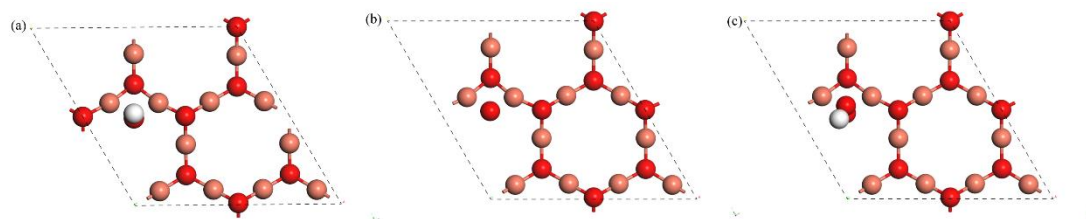

Fig. S10 The optimized adsorbed intermediates of (a) *OH, (b) *O, and (c) *OOH on active site 7 of Cl-Cu$_2$O(111).

Fig. S11 The optimized adsorbed intermediates of (a) *OH, (b) *O, and (c) *OOH on active site 8 of Cl-Cu$_2$O(111).

Fig. S12 The optimized adsorbed intermediates of (a) *OH, (b) *O, and (c) *OOH on active site 9 of Cl-Cu₂O(111).

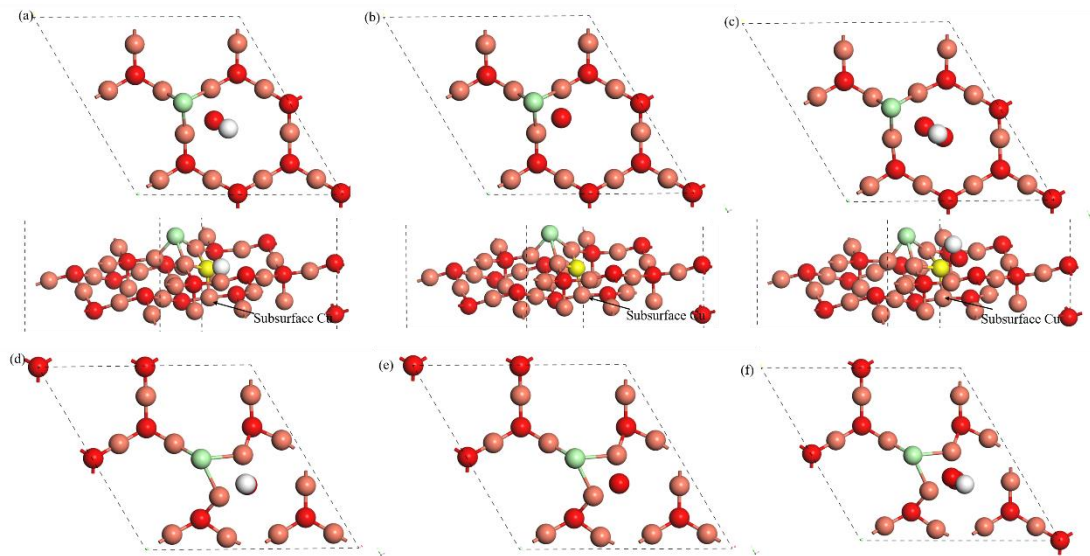**Fig. S13** The optimized adsorbed intermediates of (a) *OH, (b) *O, and (c) *OOH on active site 10 of Cl-Cu₂O(111).

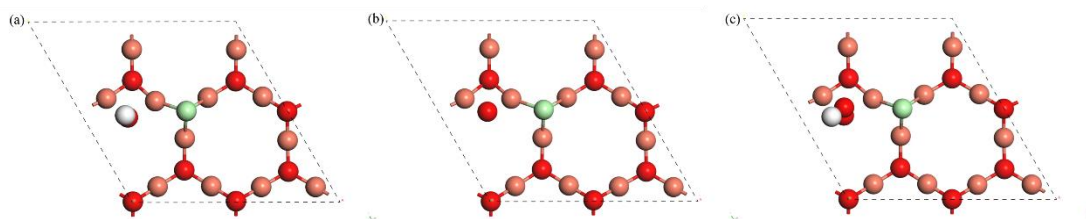**Fig. S14** The optimized adsorbed intermediates of (a) *OH, (b) *O, and (c) *OOH on active site 11 of Cl-Cu₂O(111).

Fig. S15 The optimized adsorbed intermediates of (a) *OH(2), (b) *O(3), (c) *OOH(2), (d) *OH(3), and (e) *OOH(3) on active site 1 of V_{Cu}-$Cu_2O(111)$. The coordinated O* atoms are in yellow in side views.
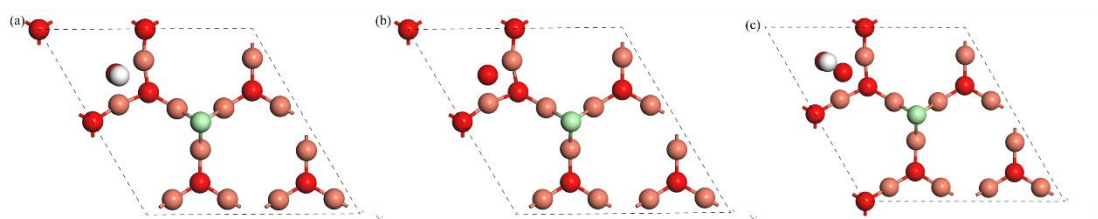

Fig. S16 The optimized adsorbed intermediates of (a) *OH, (b) *O, and (c) *OOH on active site 2 of V_{Cu}-$Cu_2O(111)$.

Fig. S17 The optimized adsorbed intermediates of (a) *OH(3), (b) *O(3), (c) *OOH(3), (d) *OH(2), (e) *O(2) and (d) *OOH(2) on active site 1 of V_{Cu}-Cl-Cu$_2$O(111). The coordinated O* atoms are in yellow in side views.

Fig. S18 The optimized adsorbed intermediates of (a) *OH, (b) *O, and (c) *OOH on active site 2 of V_{Cu}-Cl-Cu$_2$O(111).
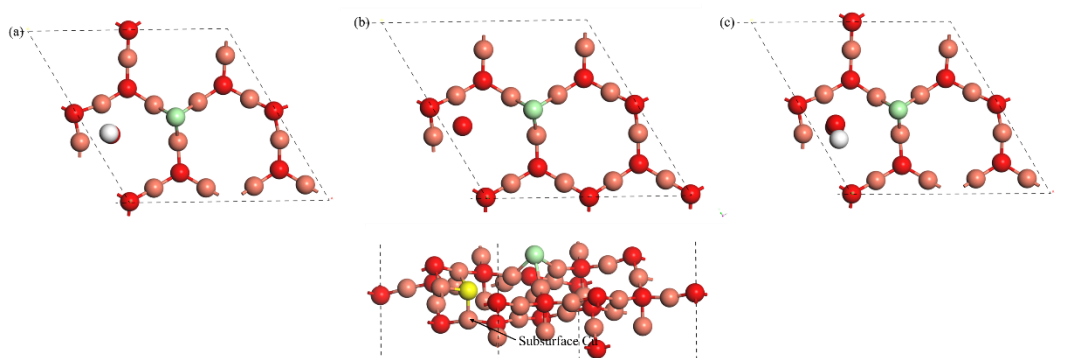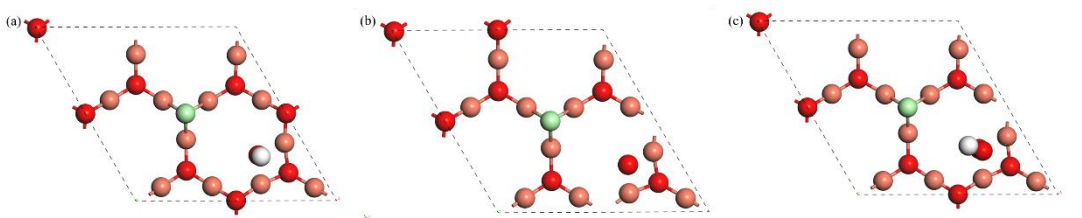

**Fig. S19** The optimized adsorbed intermediates of (a) *OH, (b) *O, and (c) *OOH on active site 3 of V_{Cu}-Cl-Cu$_2$O(111).

Fig. S20 The optimized adsorbed intermediates of (a) *OH(2), (b) *O(3), and (c) *OOH(2) on active site 4 of V_{Cu}-Cl-Cu$_2$O(111). The coordinated O* atoms are in yellow in side views.

Fig. S21 The optimized adsorbed intermediates of (a) *OH, (b) *O, and (c) *OOH on active site 5 of V_{Cu}-Cl-Cu$_2$O(111).

Table S7 Bader charge of OH absorbing at the most active site on Cu$_2$O(111), Cl-Cu$_2$O(111), V_{Cu}-Cu$_2$O(111) and V_{Cu}-Cl-Cu$_2$O(111).

surface	*OH charge (|e|)
3-Cu$_2$O(111)	-0.559
7-Cl-Cu$_2$O(111)	-0.561
2-V_{Cu}-Cu$_2$O(111)	-0.475
2-V_{Cu}-Cl-Cu$_2$O(111)	-0.505
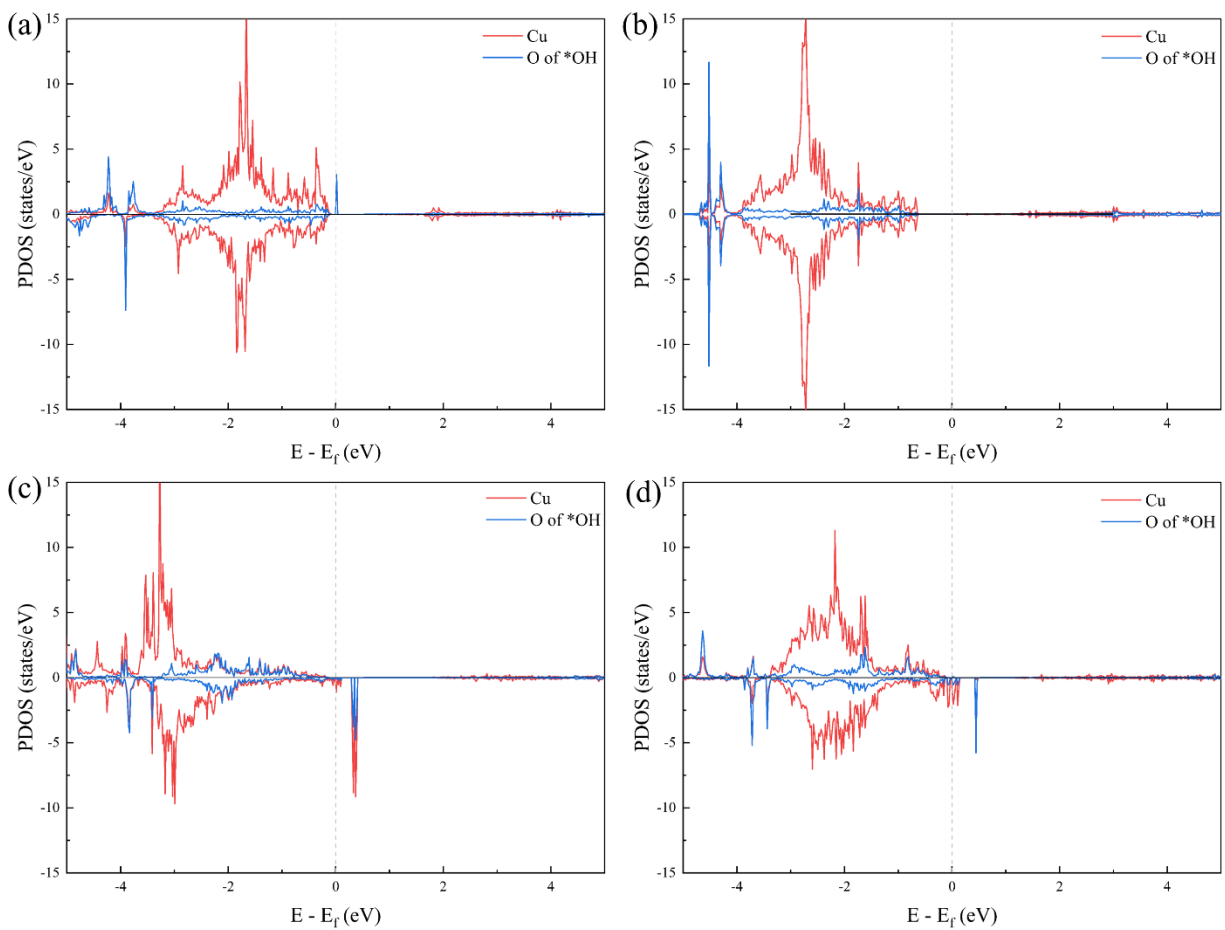
Fig. S22 The projected density of states (PDOS) of OH* absorbing at the most active site on (a) $Cu_2O(111)$, (b) $Cl-Cu_2O(111)$, (c) $V_{Cu}-Cu_2O(111)$ and (d) $V_{Cu}-Cl-Cu_2O(111)$, where the Fermi energy was set to zero (dashed line).

Table S8 Comparison of Gibbs reaction free energy changes ($\triangle G$) of each elementary step and overpotential (η) on the active sites of different $Cu_2O(111)$ surfaces with or without an implicit model.

surface	implicit solvation model	$\triangle G_{*OH}$ (eV)	$\triangle G_{*O}$ (eV)	$\triangle G_{*OOH}$ (eV)	η (V)
3-Cu$_2$O(111)	without	0.86	1.92	4.05	0.90
	with	0.64	1.70	3.48	0.54
7-Cl-Cu$_2$O(111)	without	-0.12	1.68	3.32	0.58
	with	-0.39	1.40	2.93	0.76
2-V$_{Cu}$-Cu$_2$O(111)	without	1.50	3.25	4.80	0.52
	with	1.27	2.97	4.42	0.47
2-V$_{Cu}$-Cl-Cu$_2$O(111)	without	1.57	3.26	4.82	0.46
	with	1.43	3.03	4.53	0.36

Reference

1   J. K. Nørskov, J. Rossmeisl, A. Logadottir, L. Lindqvist, J. R. Kitchin, T. Bligaard and H. Jónsson, *The Journal of Physical Chemistry B*, 2004, **108**, 17886‑17892.